Australian Journal of Basic and Applied Sciences, 7(7): 494-504, 2013
ISSN 1991-8178

Stabilizing Controller Design for Self Erecting Single Inverted Pendulum using Robust LQR

[1]Vinodh Kumar E, [2]Jovitha Jerome

[1]Department of Instrumentation and Control Systems Engineering, PSG College of Technology, Coimbatore, India-641004.
[2]Department of Instrumentation and Control Systems Engineering, PSG College of Technology, Coimbatore, India-641004.

Abstract: This paper describes the method for trajectory tracking and balancing the Self Erecting Single Inverted Pendulum (SESIP) using Linear Quadratic Regulator (LQR). A robust LQR controller for stabilizing the SESIP is proposed in this paper. The first part of the controller is a Position Velocity (PV) controller to swing up the pendulum from its hanging position by moving the pendulum left and right repeatedly until the pendulum swings up around the upright position. The second part is the stabilization controller which is obtained by the optimal state feedback control law determined using LQR to balance the pendulum around upright position. Both the dynamic and steady state characteristics of controller are investigated by conducting experiments on linear inverted pendulum system and the results are compared with the conventional double PID controller response to evaluate the effectiveness of the proposed scheme. Experimental results prove that the LQR controller can guarantee the inverted pendulum a faster and smoother stabilizing process with less oscillation and better robustness than a conventional double PID controller.

Key words: Inverted Pendulum, LQR Controller, PID Controller, Riccatti Equation, State feedback control, PV Controller.

INTRODUCTION

Inverted pendulum is a fourth order, unstable, nonlinear, multivariable, and under actuated system which can be treated as a typical control problem to study various modern control theories. It is a well established benchmark problem that provides many challenging problems to control design. According to control purposes of inverted pendulum, the control of inverted pendulum can be divided into three aspects. The first aspect that is widely researched is the swing-up control of inverted pendulum. The second aspect is the stabilization of the inverted pendulum (Jia-Jun Wang 2011). The third aspect is tracking control of the inverted pendulum (Wai *et al*. 2006, Chang *et al*. 2007). In practice, stabilization and tracking control is more useful for plenty of real time applications. There are several tasks to be solved in the control of inverted pendulum, such as swinging up and catching the pendulum from its stable pending position to the upright unstable position, and then balancing the pendulum at the upright position during disturbances, and further move the cart to a specified position on the rail. Many approaches for swinging and catching of an inverted pendulum have been proposed in the literature (see for instance, Furuta *et al*.1992, Åström *et al*. 2000). While controlling a real inverted pendulum, control engineers are faced up with several limitations and constraints. One such important limitation is that the rail has a limited length and, thus, the cart movement is limited. There are few solutions have been proposed for swing up and stabilization of a cart pendulum with a restricted travel. A nonlinear control strategy by decomposing the control law into a sequence of steps was proposed in (Wei *et al*. 1995) and (Chung *et al*. 1995) proposed a nonlinear control state controller that controls the cart position and the swinging energy of the pendulum at the same time. An energy based control law that swings up and stabilizes a cart-pendulum system with restricted travel and restricted control force was suggested in (Chatterjee *et al*. 2002). Apart from the control problem of the single rod inverted pendulum on a cart system, control aspects of other types like double inverted pendulum on a cart, the rotational single-arm pendulum and the rotational two-link pendulum have also been reported in the literature (Mason *et al*. 2008, Tao et. al, 2008). In this investigation, the model of a single rod inverted pendulum on a cart system is considered for the development of the proposed control algorithm. The goal of this contribution is to implement the target tracking and stabilizing controller for the SESIP based on the control concepts of LQR theory. The rest of this paper is organized as follows. The nominal mathematical model of an inverted pendulum system obtained from first principles is presented in Section 2. Controller design problem for both swing up and stabilization is formulated in Section 3. In section 4, design steps of PV, LQR and PID controllers are explained. Experimental results are presented in section 5 and the paper ends with the concluding remarks in section 6.

Corresponding Author: Vinodh Kumar E, Department of Instrumentation and Control Systems Engineering, PSG College of Technology, Coimbatore, India-641004.
E-mail: vinothmepsg@gmail.com

System Model:

The linear Self Erecting Single Inverted Pendulum (SESIP) consists of a pendulum system which is attached to a cart equipped with a motor that drives it along a horizontal track. The schematic diagram of inverted pendulum system is shown in Fig. 1.

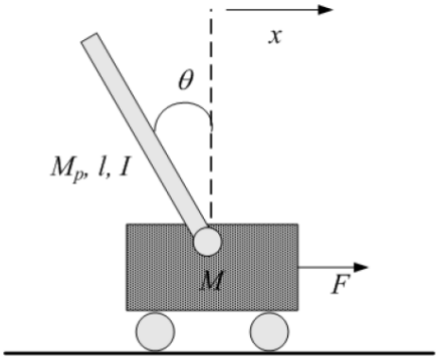

Fig. 1: Schematic of Cart-Inverted Pendulum.

The position and velocity of the cart can be changed through the motor and the track restricts the cart movement in the horizontal direction. Encoders are attached to the cart and the pivot in order to measure the cart position and pendulum joint angle, respectively (M. I Iwan Solihin *et al*. 2010). The block diagram of the overall set up is shown in Fig. 2.

Table 1: List of parameters.

Symbol	Description	Value/Unit
R	Motor armature resistance	2.6Ω
L	Motor armature inductance	0.18mH
K_t	Motor torque constant	0.00767 Nm/A
η_m	Motor efficiency	100%
K_m	Motor EMF constant	0.00767 Ns/rad
J	Rotor moment of inertia	$3.9x10^{-7}$ kgm^2
K_g	Gearbox ratio	3.71
η_g	Gearbox efficiency	100%
r_m	Motor pinion radius	$6.35x10^{-3}$ m
r_p	Position pinion radius	$1.48x10^{-2}$ m
B_{eq}	Equivalent viscous damping coefficient at motor	5.4 Nms/rad
B_p	Viscous damping coefficient at pendulum pivot	5.4 Nms/rad
l	Pendulum length from pivot to centre of mass	0.3302 m
I	Pendulum moment of inertia	$7.88x10^{-3}$ kgm^2
M_p	Pendulum mass	0.23kg
M	Cart mass	0.94kg
V_m	Motor nominal input voltage	5V

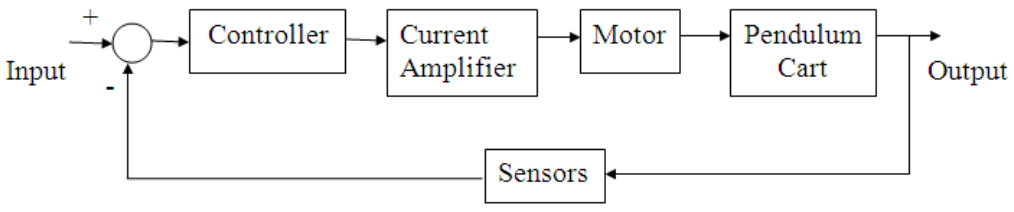

Fig. 2: Pendulum cart system block diagram.

Single Inverted Pendulum Equation of Motion:

The schematic diagram and angle definitions of SESIP are shown in Fig. 3. The single inverted pendulum (SIP) system is made of a motor cart on top of which pendulum is pivoted. The movement of the cart is constrained only in the horizontal x direction, where as the pendulum can rotate only in the x-y plane (A.A. Saifizul *et al*. 2006). The SIP system has two DOF and can be fully represented using two generalized coordinates such as horizontal displacement of the cart, x_c and rotational displacement of pendulum, α. The

nominal plant model is obtained with the assumption that the coloumb's friction applied to the linear cart and the force on the linear cart due to the pendulum's action have been neglected.

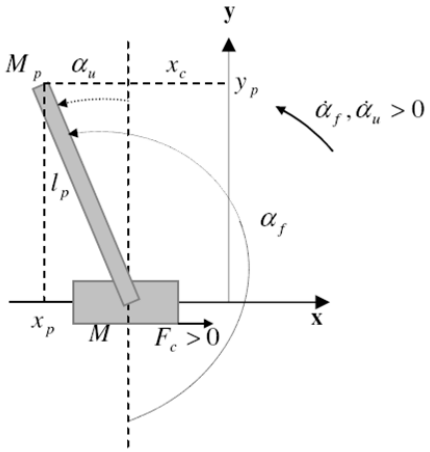

Fig. 3: SESIP Schematic.

A nonlinear equation of motion (EOM) of SIP can be obtained using Lagrange's equation.

$$\frac{d}{dt}\left[\frac{\partial L}{\partial \dot{x}_c}\right] - \frac{\partial L}{\partial x_c} = Q_{x_c} \tag{1}$$

and

$$\frac{d}{dt}\left[\frac{\partial L}{\partial \dot{\alpha}}\right] - \frac{\partial L}{\partial \alpha} = Q_{\theta} \tag{2}$$

With L= $T_T - V_T$ where T_T is total kinetic energy, V_T is total potential energy, Q_{x_c} and Q_{θ} are the generalized force applied on the coordinate x_c and α, respectively. Both the generalized forces can be defined as follows

$$Q_{x_c}(t) = F_c(t) - B_{eq}\dot{x}_c \tag{3}$$

and

$$Q_{\alpha} = -B_p\dot{\alpha}(t) \tag{4}$$

This energy is usually caused by its vertical movement from normality (gravitational potential energy) or by a spring related sort of displacement. The cart linear motion is horizontal and as such, never has vertical displacement. So, the total potential energy is fully represented by the pendulum's gravitational potential energy, as characterized below:

$$V_T = M_p g l_p \cos\big(\alpha(t)\big) \tag{5}$$

The amount of energy in a system due to its motion is measured by the kinetic energy. Hence, the total kinetic energy can be depicted as follows:

$$T_T = T_c + T_p \tag{6}$$

Where T_c and T_p are the sum of the translational and rotational kinetic energies arising from both the cart and its mounted inverted pendulum, respectively. First, the translational kinetic energy of the motorized cart T_{ct}, is expressed as follows:

$$T_{ct} = \frac{1}{2}M{\dot{x}_c}^2 \tag{7}$$

Second, the rotational kinetic energy due to the cart's DC motor, T_{cr} , can be represented by:

$$T_{cr} = \frac{1}{2}\frac{J_m {K_g}^2 {\dot{x}_c}^2}{{r_{mp}}^2} \tag{8}$$

Therefore, the cart's total kinetic energy, can be written as shown below:

$$T_c = \frac{1}{2} M_c \dot{x}_c^{\,2} \tag{9}$$

Where $M_c = M + (J_m {K_g}^2 / {r_{mp}}^2)$

The total kinetic energy of the pendulum, T_p ,is the sum of translational kinetic energy, T_{pt} and rotational kinetic energy, T_{pr} .

$$T_p = T_{pt} + T_{pr} = \frac{1}{2} M_p \dot{r_p}^{\,2} + \frac{1}{2} I_p \dot{\alpha}^2(t) \tag{10}$$

Where $\dot{r_p}^{\,2} = \dot{x_p}^{\,2} + \dot{y_p}^{\,2}$. From Figure $\dot{x}_p$ and $\dot{y}_p$ can be expressed as:

$$\dot{x}_p = \dot{x}_c - l_p \cos(\alpha(t))\dot{\alpha}(t) \tag{11}$$

and

$$\dot{y}_p = -l_p \sin(\alpha(t))\,\dot{\alpha}(t) \tag{12}$$

Substituting (22), (23),(24),(25) into (19), gives the total kinetic energy, T_T of the system as:

$$T_T = \frac{1}{2}(M_c + M_p)\dot{x}_c^{\,2}(t) - M_p l_p \cos(\alpha(t))\dot{\alpha}\,(t)$$
$$\dot{x}_c(t) + \frac{1}{2}(I_p + M_p {I_p}^2)\dot{\alpha}^2(t) \tag{13}$$

The lagrangian can be expressed using (18) and (26)

$$L = T_T - V_T$$
$$= \frac{1}{2}(M_c + M_p)\dot{x}_c^{\,2}(t) - M_p l_p \cos(\alpha(t))\dot{\alpha}\,(t)\dot{x}_c(t) + \frac{1}{2}(I_p + M_p {I_p}^2)\dot{\alpha}^2(t) - M_p g l_p \cos(\alpha(t)) \tag{14}$$

From equation (14) and (15), the non linear equation of motion can be obtained as:

$$(M_c + M_p)\ddot{x}_c(t) + B_{eq}\dot{x}_c(t) - (M_p l_p \cos(\alpha(t)))\ddot{\alpha}(t) + M_p l_p \sin(\alpha(t))\dot{\alpha}^2(t) = F_c(t) \tag{15}$$

and

$$-M_p l_p \cos(\alpha(t))\,\ddot{x}_c(t) + (I_p + M_p {l_p}^2)\ddot{\alpha}(t) + B_p\dot{\alpha}(t) - M_p g l_p \sin(\alpha(t)) = 0 \tag{16}$$

The nonlinear model can be linearized which is valid near the equilibrium point (upright pendulum) so that sin(α)≅ α, cos(α)≅ 1 and also neglecting higher order term. The linearized model is written in state space in order to allow the design of state feedback controller for upright pendulum stabilization.

$$\dot{X} = AX + BU \tag{17}$$
$$Y = CX$$

Where $X = [x_c\ \alpha\ \dot{x}_c\ \dot{\alpha}]^T$, $U = V$ and $Y = [x_c\ \ \alpha]^T$

$$A = \begin{bmatrix} 0 & 0 & 1 & 0 \\ 0 & 0 & 0 & 1 \\ 0 & \dfrac{(M_p l)^2}{q} & \dfrac{-B_{eq}(M_p l^2 + I)}{q} & \dfrac{M_p l B_p}{q} \\ 0 & \dfrac{(M + M_p)M_p g}{q} & l \quad \dfrac{M_p l B_{eq}}{q} & \dfrac{(M + M_p)B_p}{q} \end{bmatrix} \qquad B = \begin{bmatrix} 0 \\ 0 \\ \dfrac{M_p l^2 + I}{q} \\ \dfrac{M_p l}{q} \end{bmatrix}$$

The state model of the system obtained by substituting the parameters presented in Table 1 is given as:

$$\begin{bmatrix} \dot{x_c} \\ \dot{\alpha} \\ \ddot{x_c} \\ \ddot{\alpha} \end{bmatrix} = \begin{bmatrix} 0 & 0 & 1 & 0 \\ 0 & 0 & 0 & 1 \\ 0 & 2.2643 & -15.8866 & -0.0073 \\ 0 & 27.8203 & -36.6044 & -0.0896 \end{bmatrix} \begin{bmatrix} x_c \\ \alpha \\ \dot{x_c} \\ \dot{\alpha} \end{bmatrix} + \begin{bmatrix} 0 \\ 0 \\ 2.2772 \\ 5.2470 \end{bmatrix} u \tag{18}$$

$$y = \begin{bmatrix} 1 & 0 & 0 & 0 \\ 0 & 1 & 0 & 0 \end{bmatrix} \begin{bmatrix} x_c \\ \alpha \\ \dot{x_c} \\ \dot{\alpha} \end{bmatrix} \tag{19}$$

The eigen values of the system matrix are -16.2577, -4.5611, 0, 4.8426. It can be clearly seen that the open loop system has one pole in the Right Half Plane (RHP) i.e., positive pole. Therefore the system is unstable in open loop. As a consequence, in order to maintain the pendulum balanced in the inverted position, a controller is to be designed such that all the resulting closed loop poles lie in the Left Half Plane (LHP).

Formulation of Controller Design Problem:

The controller design for the inverted pendulum system is broken up into two components. The first part involves the design of a swing up controller that swings the pendulum up to the unstable equilibrium. The second part involves the design of an optimal state feedback controller for the linearized model that will stabilize the pendulum around the upright position. When the pendulum approaches the linearized point, the control will switch to the stabilizing controller which will balance the pendulum around the vertical position.

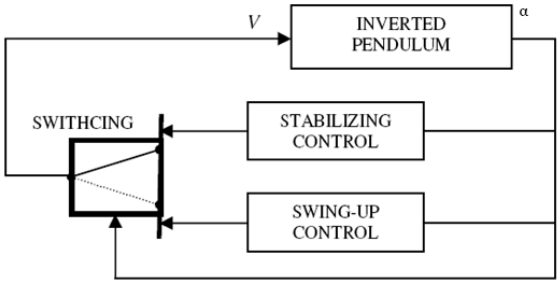

Fig. 4: Control scheme of inverted pendulum.

The control scheme of SESIP consists of two main control loops and decision making logic to switch between the two control schemes. The control scheme of the inverted pendulum is shown in Fig. 4. One control loop is a PV controller on the cart position that follows a set point designed to swing up the pendulum from the suspended to the inverted posture. The other control loop is active when the pendulum is around the upright position and consists of a Linear Quadratic Regulator maintaining the inverted pendulum in vertical position.

LQR Design Specification:

The primary objective of the LQR scheme is to catch, in a first time, "swing-up" pendulum and then to maintain it balanced in the inverted posture. The linear cart should track a desired (square wave) position set point and at the same time the controller should also minimize the control effort. The purpose of optimal control is to allow for best tradeoff between performance and cost of control. The gain of the LQR scheme is tuned to control the inverted pendulum and linear cart system to satisfy the following design requirements.

1. The pendulum angle should be regulated around its upright position and never exceed a ± 1 degree deflection.
2. Rise time $\leq$2s
3. Control effort V_m should be minimum and is not allowed to reach the saturation level.

Controller Design:

PV Controller:

This controller aims at swinging up the pendulum from rest (θ=180^0=-180^0) while keeping the cart travels within the limited horizontal distance. Many different control algorithms can be used to perform the swing up control such as, trajectory tracking, rectangular reference input swing up type and Pulse Width Modulation (PWM), in a controlled manner that the energy is gradually added to the system to bring the pendulum to the inverted position. In this work, a PV controller is used because of its simple structure, effectiveness and easy tuning. The block diagram representation of swing up controller is shown in Fig. 5. The proportional velocity

position controller for servo plant introduces two corrective terms. One is proportional (K_{p_c}) to the cart position error while the other is proportional (K_{d_c}) to the cart velocity. The resulting PV control law is given as:

$$V_m(t) = K_{p_c}\big(x_d(t) - x_c(t)\big) + K_{v_c}\left[\frac{d}{dt}x_c(t)\right] \tag{20}$$

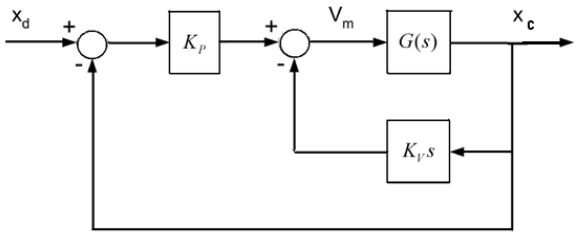

Fig. 5: Block diagram of PV controller.

The closed loop transfer function of the cart servo can be expressed as:

$$\frac{X_c(s)}{X_d(s)} = \frac{K_p G(s)}{1+K_p G(s)+sK_v G(s)} \tag{21}$$

This leads to a second order system as follows:

$$\frac{X_c(s)}{X_d(s)} = \frac{1.6\,K_p}{s^2+s(12.23+1.6K_v)+1.6K_p} \tag{22}$$

The desired performance is ζ=0.59 and ω=26 rad/s. Comparing characteristic equation in (19) with the standard second order form:

$$s^2 + 2\zeta\omega s + \omega^2 = 0 \tag{23}$$

the PV controller gains are obtained as $K_p = 274.62$ and $K_v = 5.53$.

Switching Algorithm:

A transition algorithm is designed to switch from swing-up controller to stabilizing controller. This is performed by smooth conditional switching that can be expressed as follows:
If $|\alpha|>25^0$, only swing-up control is active.
If $|\alpha|<20^0$, only stabilizing control is active.
If $20^0 \leq|\alpha|\leq25^0$, swing-up and stabilizing control signal are averaged/weighted. The last condition is made as transition region to avoid what known as hard switching.

LQR Controller:

The LQR method is a powerful technique for designing controllers for complex systems that have stringent performance requirements and it seeks to find the optimal controller that minimizes a given cost function (Aamir *et al*. 2010). The cost function is parameterized by two matrices, Q and R, that weight the state vector and the system input respectively. LQR method is based on the state-space model and to find the control law, a matrix Riccati equation is first solved, and an optimal feedback gain, which will lead to optimal results evaluating from the defined cost function (performance index), is obtained. In this paper, the state feedback controller is designed using the linear quadratic regulator and the linear model of the system. Briefly, the LQR/LTR theory says that, given a n^{th} order stabilizable system

$$\dot{x}(t) = Ax(t) + Bu(t), \quad t \geq 0, \;\; x(0) = x_0 \tag{24}$$

Where $x(t)$ is the state vector and u(t) is the input vector, determine the matrix $K \in R^{n\times m}$such that the static, full state feedback control law,

$$u(t) = -Kx(t) \tag{25}$$

satisfies the following criteria,

a. the closed-loop system is asymptotically stable
b. the quadratic performance functional

$$J(K) = \frac{1}{2}\int_0^{\infty}[x^T(t)Qx(t) + u^T(t)Ru(t)]\,dt \quad (26)$$

is minimized. Q is a nonnegative definite matrix that penalizes the departure of system states from the equilibrium and R is a positive definite matrix that penalizes the control input (Desineni *et al*, 2003). The solution of the LQR problem can be obtained via a Lagrange multiplier based optimization technique and is given by

$$K = R^{-1}B^TP \quad (27)$$

Where P∈ $R^{n\times m}$ is a nonnegative definite matrix satisfying the matrix Riccati Equation,

$$A^TP + PA + Q - PBR^{-1}B^TP = 0 \quad (28)$$

Given the plant (37) and the performance index (39), the following LQR design algorithm is used to determine the optimal state feedback.
Step 1: Solve the matrix algebraic Riccati equation (ARE)

$$-PA - A^TP - Q + PBR^{-1}B^TP = 0 \quad (29)$$

Step 2: Determine the optimal state x*(t) from

$$\dot{x}^*(t) = [A - BR^{-1}B^TP]x^*(t) \quad (30)$$

with initial condition $x(t_0) = x_0$
Step 3: Obtain the optimal control u*(t) from

$$u^*(t) = -R^{-1}B^TPx^*(t) \quad (31)$$

Step 4: Obtain the optimal performance index from

$$J^* = \frac{1}{2}x^{*'}(t)Px^*(t) \quad (32)$$

The weighting matrices Q and R are important components of an LQR optimization process. The compositions of Q and R elements have great influences on system performance. Different approaches have been suggested for the selection of weighting matrices. In this work, for the selection of weighting matrices Bryson's rule is followed (Omer *et al*. 2010). A reasonable simple choice for the matrices Q and R by Bryson's rule is given by

$$Q_{ii} = \left[(t_f - t_0) \times \max\,(x_i(t_f))^2\right]^{-1} \quad (33)$$

$$R_{ii} = \left[(t_f - t_0) \times \max\,(u_i(t_f))^2\right]^{-1} \quad (34)$$

The number of elements of Q and R matrices are dependent on the number of state variable (n) and the number of input variable (m), respectively. The diagonal-off elements of these matrices are zero for simplicity. If diagonal matrices are selected, the quadratic performance index is simply a weighted integral of the squared error of the states and inputs.

PID Controller Design:

In this section the design of PID controller for stabilizing the inverted pendulum is presented in order to make a comparison between the performances of proposed LQR and PID controllers. Several methods have been proposed to control the inverted pendulum, such as traditional PID control, fuzzy control and genetic algorithm optimizing control. Although a lot of control algorithms are researched in the designing of the inverted pendulum system controller, PID controller is still the most widely used controller structure in the realization of a control system. However, the inverted pendulum system is a one input and two output system which contradicts to the one input and one output control characteristic of the single PID controller (Wende *et*

al. 2012). The steady state error of the pendulum angle using single PID controller results in the one direction displacement of the cart. The displacement of the cart cannot be controlled very well because the PID controller can control only one variable, and the cart position control problem is ignored and only pendulum angle is focused. So the double PID control structure is used to solve the multi-output problem. Block diagram of the designed double-PID control method is shown in Fig. 6.

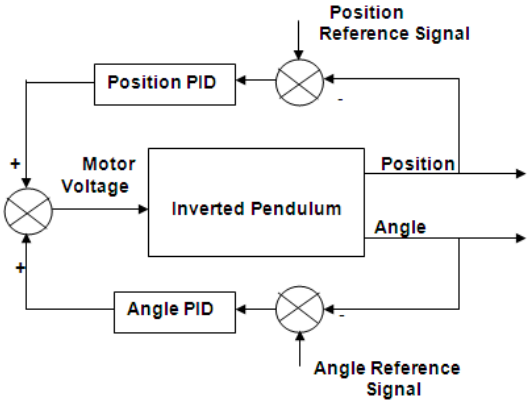

Fig. 6: Block diagram of double PID control method.

PID–I controls the cart position and PID-II controls the pendulum angle. The output of both the PID controllers are summed together to produce a control input to the pendulum system. Using Ziegler-Nichols technique, the parameter values of both the PIDs are determined. The control parameters are [Kpp=40, Kpi=25, Kpd=20; Kap=60, Kai=85, Kad=9].

Experimental Results:

In order to show the practical effectiveness of the proposed scheme, experiments are conducted using Quanser IP-02 inverted pendulum system. The snapshot of the experimental set up is shown in Fig. 7. Firstly, the experimental results of two phases of swing up and stabilizing modes are presented. Secondly, the performance of robust LQR controller design is compared with a double PID controller performance. Real time experiment configuration consists of computer with MATLAB, Simulink, Q8 data acquisition board and Quanser IP02 Linear inverted pendulum module. Some hardware limitations are considered in the controller design for the pendulum system. The Digital-to-Analog voltage for data acquisition board is limited between -10 V and 10 V. The safety watchdog is turned on where the allowable cart displacement is 0.35 *m* from the centre of the track. When the pendulum or cart touches the limit switch, the control process is aborted. The Simulink block diagram of the overall control design is shown in Fig 8.

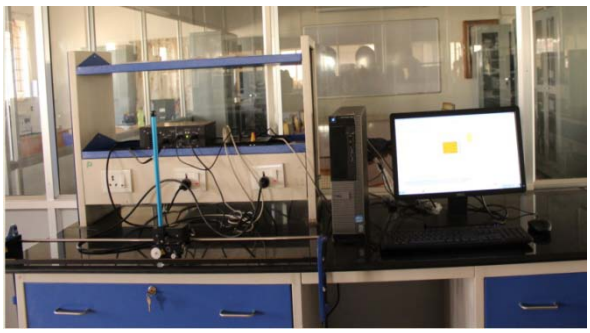

Fig. 7: Snapshot of experimental setup.

The controller gains of a state feedback controller are determined using the weighting matrices of linear quadratic regulator. The following weighting matrices are selected based on Bryson's rule for the calculation of gain K.

$$Q = \begin{bmatrix} 0.5 & 0 & 0 & 0 \\ 0 & 5.5 & 0 & 0 \\ 0 & 0 & 0 & 0 \\ 0 & 0 & 0 & 0 \end{bmatrix} \qquad R = [0.0003]$$

Using the system model from (31) and the above weighting matrices, the state feedback controller gains obtained for robust LQR controller is

$$K = [-44.72 \quad 200.8 \quad -49.77 \quad 27.38]$$

Fig. 9 shows the output of the swing up controller which is able to bring the pendulum to upright position in approximately 7 sec. The swing up controller takes approximately 12 swings before the pendulum reaches close to vertical position. The velocity of the pendulum angle reaches the maximum value of 650deg/s to -650deg/s during swing up phase as shown in Fig. 10.

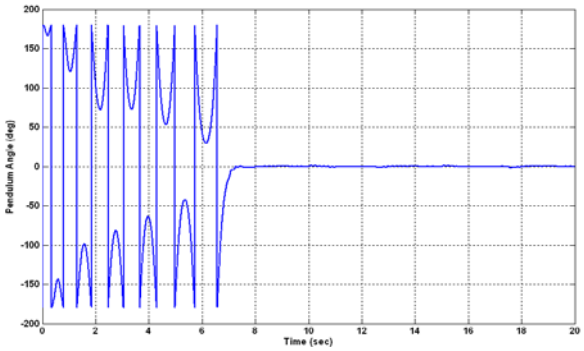

Fig. 8: Pendulum angle during swing up phase.

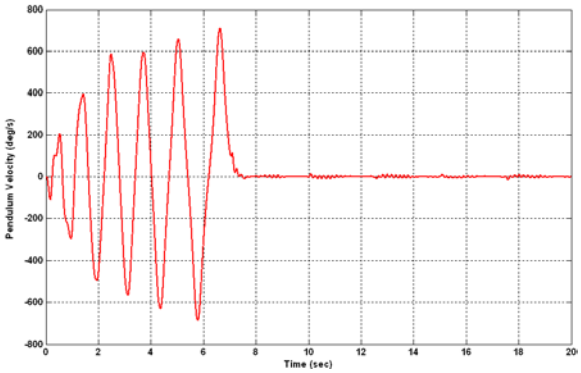

Fig. 9: Pendulum Velocity.

During the swing up phase, the control signal is larger than the control signal in the stabilizing mode. This is relevant because large amount of energy is required to swing the pendulum from downward position to its upright position and the small amount of energy is only required to stabilize the pendulum. The control signal applied to the cart is shown in Fig. 11. Even though the initial control signal during swing up phase reaches the maximum saturation level, the magnitude of control voltage to the motor is reduced well below 3.3V after the pendulum reaches the upright position. The control input varies between 3.25V to -3.25V after the swing up phase. The control output begins to decrease when the pendulum is close to the upright position because the control output is based on the difference between the energy of the system and the desired value.

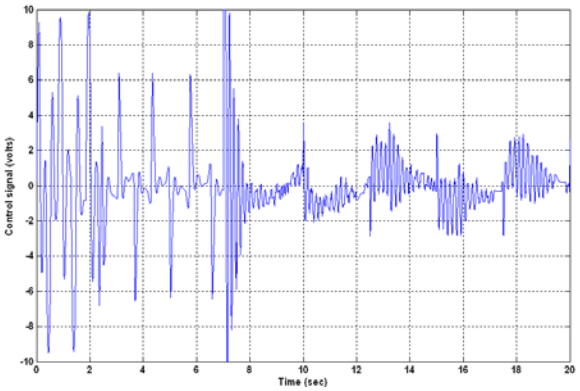

Fig. 10: Control Signal.

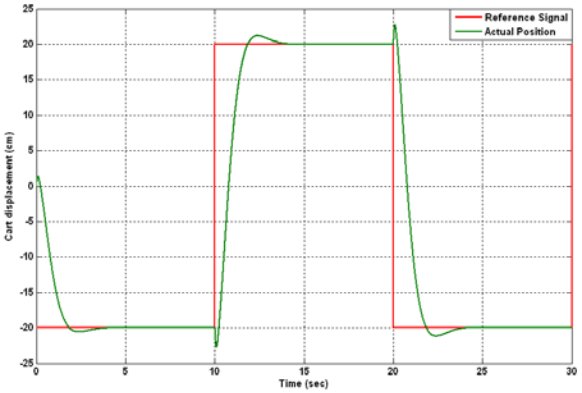

Fig. 11: Cart Position.

The trajectory tracking ability of the controller in the form of cart position response for the given square wave reference signal is shown in Fig. 12. From Fig. 12, it is observed that the overshoot of the system is less than 5 percentage, which satisfies the performance criteria mentioned in the controller specification.

Disturbance Rejection:

The disturbance rejection ability of the controller strategy is explained in this section. After the pendulum swing up and stabilization phase, disturbance is introduced into the pendulum at 15 second as shown in Fig. 13. The zoomed view of angle response is shown in Fig. 14 to highlight the magnitude of deviation in angle. The magnitude of pendulum angle deviates to 4 deg when the disturbance signal is introduced. Furthermore, as seen in Fig. 15 the magnitude of corresponding control signal applied to cart during disturbance varies between -6V to 6Vwhich is lesser than the saturation value given in the controller specification.

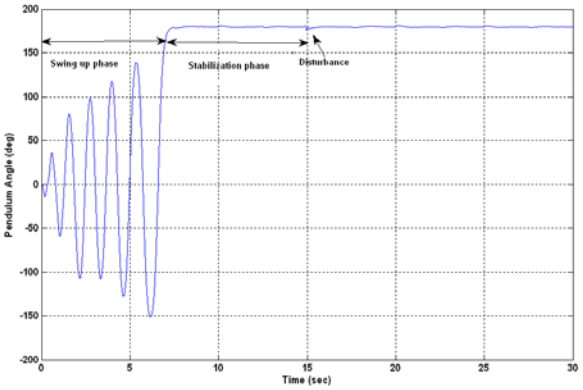

Fig. 12: Pendulum Angle with external disturbance.

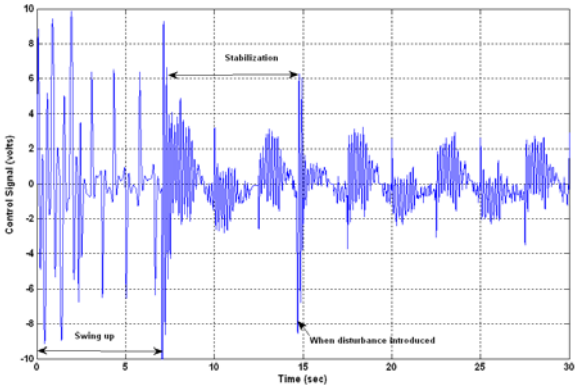

Fig. 13: Control signal applied to cart.

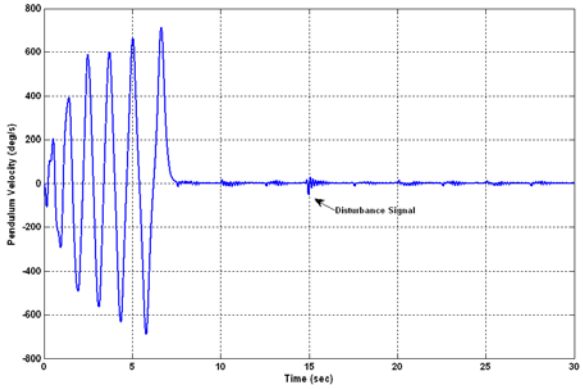

Fig. 14: Pendulum velocity.

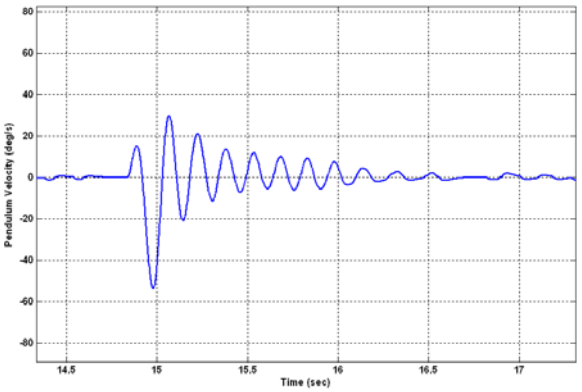

Fig. 15: Zoomed view of pendulum velocity.

Fig. 16 and 17 show the pendulum angle velocity and zoomed of the same during external disturbance, respectively. The controller is able to reduce the oscillation in less than 2 seconds which makes the pendulum to maintain its upright position to track the given signal.

Dynamic Performance Assessment of LQR and PID Controllers:

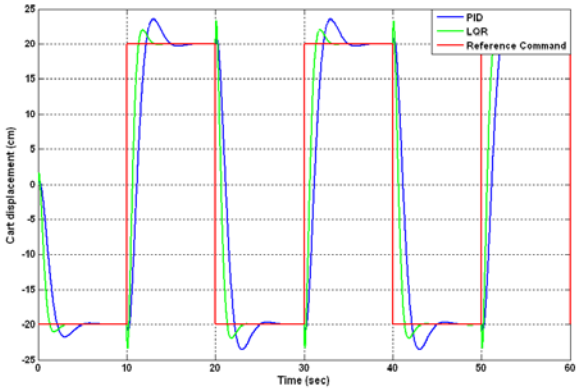

Fig. 16: Cart position response.

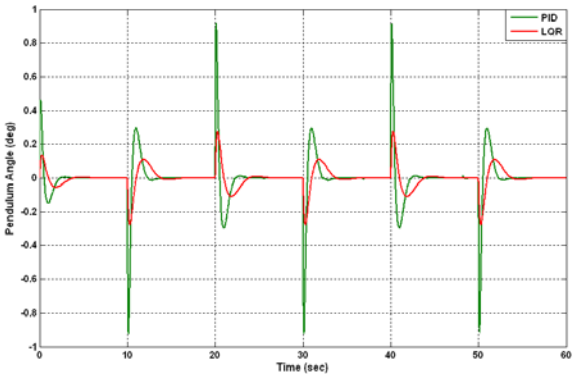

Fig. 17: Pendulum angle response.

Dynamic performance indices such as rise time, settling time and overshoot are chosen to evaluate the performance of both LQR and PID controllers for the response of cart position and pendulum angle. Fig. 19 and Fig. 20 show the response of cart position and pendulum angle, respectively. Based on the performance indices tabulated in Table 2 and Table 3, it is worth to note that the LQR controller has less rise time and reaches the set point quickly compare to conventional double PID. It is also characterized by a reduced overshoot and short delay time. In summary, for dynamic response, the inverted pendulum controlled by LQR controller 1) balances faster because of the shorter settling time; 2) has better robustness due to less maximum overshoot. So, the LQR controller can guarantee the inverted pendulum system a better dynamic performance than a conventional double PID.

Table 2: Performance Indices of Cart position.

Time domain parameter	PID	LQR
Rise Time (sec)	2.1	1.6
Settling Time (sec)	5.1	2.7
Overshoot (percentage)	15	8

Table 3: Steady state performance of PID and LQR controller.

Performance Index	PID	LQR
Pendulum angle oscillation amplitude	1.8 deg	0.3deg
Pendulum angle oscillation frequency	0.55Hz	0.43Hz

Conclusion:

A complete design and implementation of robust LQR controller to stabilize the inverted pendulum in the upright position has been described in this paper. A linear model of the SESIP has been obtained using Euler-Lagrange energy based method. The optimal weights of LQR controller have been obtained to tune the controller output which in turn modifies the output to satisfy the design criteria. The robustness property of the controller has been demonstrated by maintaining the pendulum angle with reduced oscillation when the disturbance is introduced into the system. Experimental results show that the steady state performance of the proposed LQR controller has smaller oscillation amplitude than that of the double PID controller. The control scheme not only had good dynamic performance, but also had robustness to external disturbance. As a future work, further improvement can be made on the LQR controller design by considering friction compensation to further reduce the oscillation amplitude and frequency.

REFERENCES

Aamir, H.O.A., O.A. Martino and W.D. Matthew, 2010. New Approach for Position Control of Induction motor, *45th Universities Power Engineering Conference*.

Åström, K.J., K. Furuta, 1995. Swinging up a pendulum by energy control, *Automatica*, 36(2): 287-295.

Chang, L.H., A.C. Lee, 2007. Design of nonlinear controller for bi-axial inverted pendulum system, *IET Control Theory and Application*, 1(4): 979-986.

Chatterjee, D., A. Patra and H.K. Joglekar, 2002. Swing-up and stabilization of a cart-pendulum system under restricted cart track length, *Systems Control. Letter*, 47(11): 355-364.

Chung, C.C. and J. Hauser, 1995. Nonlinear control of a swinging pendulum, *Automatica*, 31(6): 851-862.

Desineni, S.N., 2003. Optimal Control Systems, CRC press.

Futura, K., M. Yamakita and S. Kobayashi, 1992. Swinging up control of inverted pendulum using pseudo state feed-back, *J. Syst. Control Eng.*, 206(14): 263-269.

Jia-Jun, W., 2011. Simulation studies of invertedpendulum based on PID controllers, *Simulation Modeling Practice and Theory*, 19: 440-449.

Mahmud, I.S., A. Rini, 2010. Particle SwamOptimization for Stabilizing Controller of a Self-erecting Linear Inverted Pendulum, *International Journal of Electrical and Electronic Systems Research*.

Mason, P., M. Broucke, B. Piccoli, 2008. Time optimal swing-up of the planar pendulum, *IEEE Transactions on Automatic Control*, 53(8): 1876-1886.

Nenad, M., T. Boris, 2006. Swinging up and Stabilization of a Real Inverted Pendulum, IEEE Transactions on Industrial Electronics, 53(2): 631-639.

Omer, O., C. Levent, U. Erol, 2010. A Novel Method of selection of Q and R Matrices in the theory of Optimal Control, International Journal of Systems Control, 1(2): 84-92.

Saifizul, A.A., Z. Zainon, N.A. Abu Osman, C.A. Azlan and U.F.S.U. Ibrahim, 2006. "Intelligent Control for Self Erecting Inverted Pendulum Via Adaptive Neuro-fuzzy Inference System", *American Journal of Applied Sciences*, 3(4): 1795-1802.

Tao, C.W., J.S. Taur, T.W. Hsieh, C.L. Tsai, 2008. Design of a fuzzy controller with fuzzy swing-up and parallel distributed pole assignment schemes for an inverted pendulum and cart system, *IEEE Transactions on Control Systems Technology*, 16(6): 1277-1288.

Wai, R.J., L.J. Chang, 2007. Adaptive stabilizing and tracking control for a nonlinear inverted-pendulum system via sliding-mode technique, *IEEE Transactions on Industrial Electronics*, 53(2): 674-692.

Wende Li, Hui Ding, Kai Cheng, 2012. An Investigation on the Design and Performance Assessment of double-PID and LQR Controllers for the Inverted Pendulum, *UKACC International Conference on Control.*

Wei, Q., W.P. Dayawansa and W.S. Levine, 1995. Nonlinear controller for an inverted pendulum having restricted travel," *Automatica*, 31(6): 841-850.